Heat Exchanger Design and Optimization for Industrial Applications

Eman Mohamed Ismail[1], Sara Jumah Flayh[2], Murtadha SaeedMohammed[3], Karrar Saeed Mohammed[4]

[1]Department of Mechanical Engineering, Faculty of Engineering, University of Misan, Amarah, Iraq. Email: eman.mohamed@uomisan.edu.iq
[2]Department of petroleum Engineering, Faculty of Engineering, University of Misan, Amarah, Iraq Email: sarajumah@uomisan.edu.iq .
[3]Department of Mechanical Engineering, Faculty of Engineering, University of Misan, Amarah, Iraq. Email: murtadha.saeed@uomisan.edu.iq
[4]Department of Medical Physics,Almanara ,College for medical Sciences Email: karar.s.mohammed@uomanara.edu.ia

This study investigates the thermal performance of various inserts and tubes in heat exchangers for laminar and turbulent flows. Comparisons between plain tubes, plain tapes, and specialized inserts (PT-SCA, PT-SCR, PT-HW) reveal distinct thermal enhancement factors. Plain tapes exhibit superior heat transfer due to increased whirl flow, while PT-SCA disrupts primary flow, generating secondary flow and enhancing performance. PT-SCR's specific geometries promote turbulence, significantly improving heat transmission. PT-HW stands out for high turbulence near the tubing wall. Deviations between analytical and experimental values highlight potential enhancements ranging from 0.9866 to 1.0147 times for turbulent flows and 1.0090 to 1.0147 times for laminar flows, emphasizing opportunities to optimize industrial heat exchangers.

Keywords: Thermal Enhancement, Heat Transfer Efficiency, Insert Designs, Laminar and Turbulent Flows, Industrial Heat Exchangers

1. Introduction

Effective heat exchange is a crucial component that impacts many applications' performance, energy usage, and sustainability as a whole in the context of industrial operations (Wang, 2020). Heat exchangers are essential parts of many different businesses since they are the foundation of thermal management systems. These apparatuses enable the thermal energy to be transferred between fluids for recovery, heating, or cooling. In many industrial sectors, improving energy efficiency, cutting operating costs, and lessening environmental effect now depend heavily on the design and optimization of heat exchangers.

The need of creative heat exchanger design cannot be emphasized as industries continue to adapt and seek ever-higher levels of efficiency (Wang Q. C., 2022). Advanced materials, complex geometries, and advanced modelling approaches are all being explored by engineers and researchers in an effort to achieve the best possible thermal performance, cost-effectiveness, and environmental responsibility (Wang R. Z., 2021). This improvement quest is in line with the larger global goals of energy conservation and sustainable development. As a result, heat exchanger design and optimization have become dynamic fields of study that combine materials science, fluid dynamics, and thermodynamics concepts to answer the ever-changing issues encountered by modern industry (Xu, 2023).

1.1 Heat Transfer Enhancement

Raising the heat transfer coefficient is the goal of heat transfer augmentation, a technique for improving the efficiency of heat transfer systems. Common applications of heat transfer methods include process industries, thermal power plants, HVAC systems, freezers, spacecraft and automobile radiators, and many more (Xu Y. Z., 2021). The goal of achieving a high rate of heat transfer with minimal pumping power while simultaneously making the heat exchanger small has been the subject of several attempts (Zhang, 2020). Introducing a disturbance to the fluid flow can improve the heat transfer rate by disrupting the viscosity and thermal boundary layers. Similarly, the cost of pumping electricity will rise as a result of the enormous growth in pumping capacity (Zhang Y. S., 2022). To get the most out of the present heat exchanger while keeping the pumping power consumption to a minimum, several methods for improving heat transfer have been used in the past few years.

There are likely to be three main types of heat exchanger augmentation methods: active, passive, and compound (Zhou, 2020). Unlike the passive approach, which does not require any external power input, the active method does employ some external power as an input to augment heat transmission. When active and passive techniques are combined, the result is a hybrid approach known as a compound method (Zhou Y. W., 2021). There aren't many uses for complex development, which is a component of the compound technique.

1.2. Industrials applications

Applications that employ technology to increase the productivity and efficiency of tasks deemed industrial are known as industrial applications (Zhu, 2020) . These are regarded as industrial uses. The applications under consideration here are regarded as industrial applications. In terms of the applications that are currently being investigated, they are considered to be manufacturing applications.

Some common industrial applications include:

- Manufacturing:

Industrial robots are employed in many different production processes, such as painting, welding, and assembling. They may contribute to increased safety and productivity.

- Process control:

Industrial operations including flow, pressure, and temperature are monitored and managed using industrial sensors and controls. They may assist in making sure that procedures are carried out effectively and efficiently.

- Energy management:

Systems for managing industrial energy usage are used to keep an eye on and control it. They can contribute to improved sustainability and lower energy costs.

- Water treatment:

Wastewater and other industrial water sources are treated by industrial water treatment systems. They can contribute to enhancing public health and preserving the environment.

- Pollution control:

Systems for controlling industrial pollution are used to lessen the pollutants that industrial operations emit into the air and water. They can support better public health and environmental protection.

These are but a handful of the numerous ways that technology is used in industry. We may anticipate seeing even more creative and practical use of technology to enhance industrial processes as it develops.

2. Literature review

Chen et al. (2019) centred on plate-fin heat exchangers and suggested a multi-objective genetic algorithm-based optimisation technique based on entropy generation minimization. The research emphasises the importance of entropy generation as an optimisation criterion with the goal of reducing irreversibility in the system. A reliable method for concurrently optimising competing goals, such as maximising heat transfer and minimising pressure loss in plate-fin heat exchangers, is provided by the multi-objective genetic algorithm (Chen, 2019) .

Cui et al. (2020) We out a thorough analysis of experimental and computational research on shell-and-tube heat exchangers with helical baffles. The study sheds light on the most recent advancements in our knowledge of the fluid dynamics and heat transport properties connected to helical baffles. The authors enhance our comprehension of the intricate flow patterns and heat transfer mechanisms in these heat exchangers by merging numerical simulations with experimental validations (Cui, 2020).

Li et al. (2018) focused on the development and improvement of plate-fin heat exchangers for heavy-duty diesel engines' waste heat recovery. The study highlights how crucial it is to maximise plate-fin shapes in order to improve heat recovery effectiveness. The authors provide insightful information on the possible uses of plate-fin heat exchangers in the context of sustainable energy practices by concentrating on waste heat utilisation in heavy-duty diesel engines (Li, 2018).

Li et al. (2019) investigated the use of hybrid optimisation methods in the design and optimisation of microchannel heat sinks for high-heat-flux LED packages. The study emphasises how important microchannel heat sinks are for handling the heat problems that come with high-heat-flux LED applications. The hybrid optimisation techniques show how well they work at striking a compromise between conflicting goals, such minimising pressure drop and increasing heat dissipation (Li L. L., 2019).

Tlili et al. (2020) centred on applying response surface methods to the multi-objective optimisation of a plate and fin heat exchanger using hybrid nanofluids. The study looks at using hybrid nanofluids to improve the efficiency of heat transmission. The authors emphasise the potential advantages of adopting hybrid nanofluids in plate and fin heat exchangers by optimising many competing goals, such as maximising heat transfer and minimising pumping power, by applying response surface technique (Tlili, 2020).

3. Technical Details of Plain Tapes

The fabrication portion of plain tape and different cut tapes is covered in this section. Below is a discussion of the technical specifications for PT and variation cut cassettes:

i. Length: it is the separation between a simple tape's two ends.

ii. Width Ratio (WR): It is the proportion of the cut width (w) to the plain tape width (W).

iii. Depth Ratio (DR): It is the proportion of the plain tape's width (W) to the cut depth (de).

The majority of writers employed de and pitch in the range of (2 to 15mm) and (40 to 210mm) to improve heat transmission, according to the literature. Thus, the current work uses a depth of cut of de = 6 mm and a pitch of 165 mm to investigate the impact of heat transfer augmentation.

3.1. Fabrication Of Plain Tapes

For the trial run, we utilised 3 mm thick, 23 mm wide, 2000 mm long, and 165 mm pitch aluminium tapes.

3.1.1. Plain Tape Step Cut Arc

Figure 1 depicts the dimensions of a simple tape step cut arc in both its photographic and geometrical views. The copper tube was designed to fit a simple tape step cut arc with dimensions of 18mm overall width, 2000mm length, and a pitch of 165mm. This arc was used for experiments.

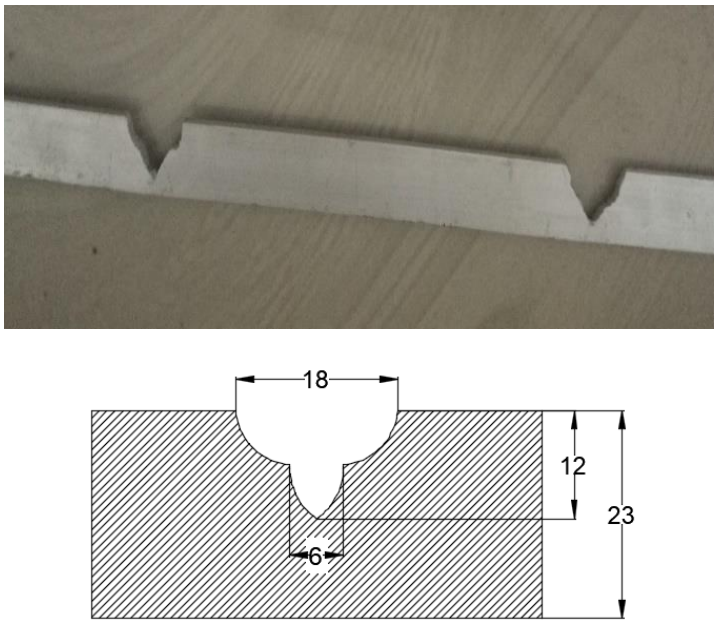

Figure 1: Photographic view and geometrical view of plain tape step cut arc

3.1.2. Plain Tape Step Cut Rectangle

Figure 2 displays the dimensions of a simple tape step cut rectangle in both its photographic and geometrical views. For the trials, the copper tube was sized to fit a simple tape step cut rectangle that was 18 mm wide, 2000 mm long, and had a pitch of 165 mm.

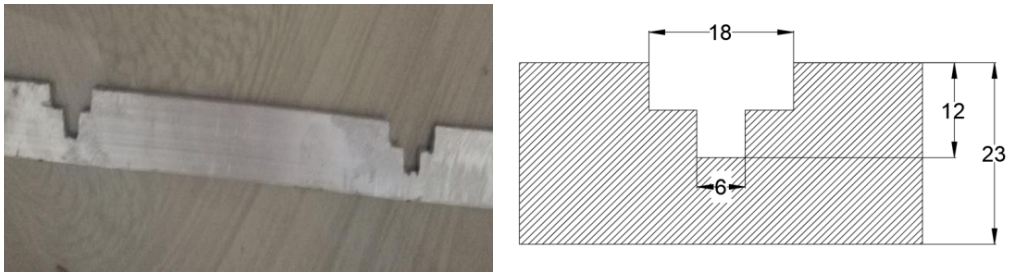

Figure 2: Photographic view and geometrical view of plain tape step cut rectangle

3.1.3. Plain Tape Horizontal Wing Cut

Pictured in Figure 3 are the geometrical and photographic views, as well as the parameters, of a simple tape horizontal wing cut. In order to conduct the research, the copper tube was sized to suit the 18mm x 6mm, 2000mm long, and 165mm pitch plain tape horizontal wing.

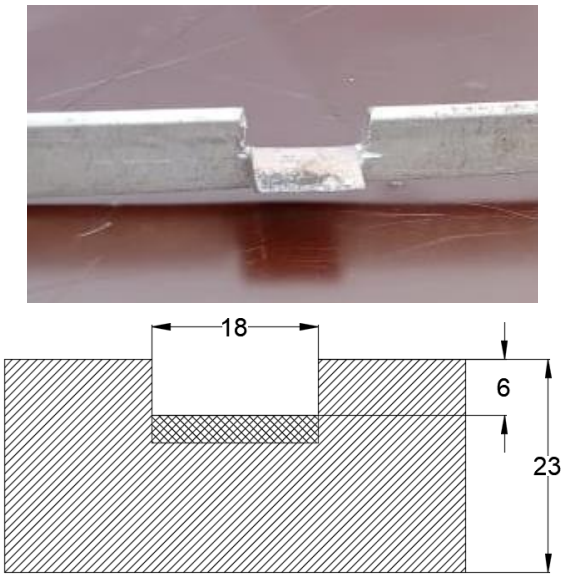

Figure 3: Photographic view and geometrical view of plain tape horizontal wing cut

4. Experimental Setup & Procedure

4.1. Heat Exchanger Specifications

There is a test section, a relative metre, tanks for hot and cold water, and pumps for both the test and the cooling water that make up the heat exchanger. Two concentric tubes make up the exchanger; one tube carries hot water (di=25 mm, L=2000 mm), while the other carries cold water (Do=54.5 mm, L=2000 mm). Two layers of asbestos cable are twisted around the annulus tube, and then it is lined with glass wool that is approximately 40 mm thick. This provides good protection for the annulus tube. To further decrease heat loss, two more layers of asbestos cable are woven.

Three adjusted Rota meters, each with a flow scope of 0 to 2 LPM (laminar flow), are utilized to compute the flow pace of hot and cold fluids with an exactness of ±0.1 LPM. Eight computerized pointers and RTD Pt 100 adjusted temperature sensors of type ±0.1 are used for temperature estimation on both the hot and cold water sides. Two sensors are utilised and the average temperature is taken into account for precise temperature measurement. Similarly, the cold-water side uses a single entrance sensor in addition to two output sensors to provide precise readings of the cold-water temperature. The experimental setup is illustrated schematically in Figure 1 and visually in Figure 2, respectively.

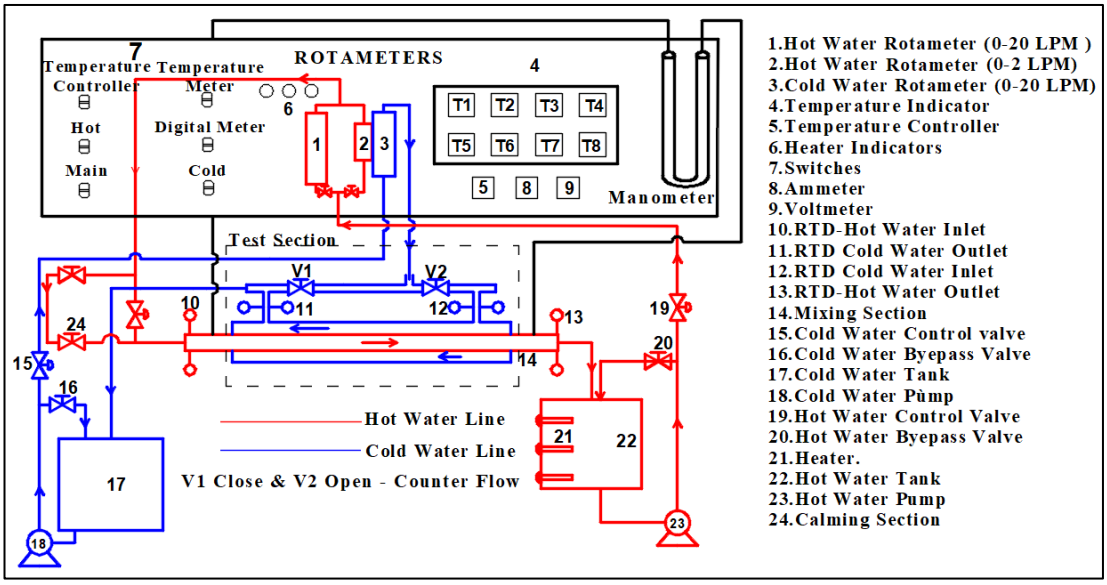

Figure 4: Schematic diagrams for counter flow double pipe heat exchanger

4.2. Experimental Procedure

At the outset, you turn on the electric heater and use the temperature controller to set the temperature to your liking. Turn on the hot water, adjust the pressure using the bypass valve in the test section, and then direct the hot water to the internal test tube using a rotating valve. In laminar flow, hot water is sent through the 0 to 2 LPM Rotameter, whereas in turbulent flow, it is directed through the 0 to 20 LPM Rotameter. A control valve directs the cold water to flow counter-clockwise to the hot water, while a by-pass valve allows any excess cold water to return to the tank. This process begins by pumping cold water from a cold-water tank.

By the end of the first hour and twenty-five minutes of the second run, we had reached steady state. The intake temperatures on the hot water side are maintained at 53±1°C, while on the cold water side they are 30±1°C. At room temperature, the cold water runs continuously at 10LPM, while the hot water's flow rate may be varied from 0.5 to 1.5LPM for laminar flow and from 2 to 8LPM for turbulent flow, with increments of 0.5LPM for each. Once the temperature of the hot or cold water reaches a constant state, only then are the intake and outflow temperatures recorded. The removal of air bubbles from the manometer ensures that the liquid levels in both limbs are identical when the flow is halted during pressure drop measurement. By adjusting the hot water flow rates, pressure drop measurements are taken under laminar and turbulent flow conditions once the system reaches steady state. For every flow rate in the plain tube and subsequently with the addition of PT, PT-SCA, PT-SCR, and PT-HW in turbulent and laminar settings, data on heat transfer and friction factor are recorded.

5. Heat Transfer

What follows is an overview of the data reduction technique for the computed results.

When using cold water to generate heat, the above equation must be followed:

$$Qc = m_c C_{pc} (T_{c1} - T_{c2}) \quad (1.1)$$

Heat transferred from the hot water is given by Equation (1.2).

$$Qh = m_c C_{pc} (T_{h1} - T_{h2}) \quad (1.2)$$

The level of heat loss among hot and cold-water side in the current heat exchanger is given in Equation (1.3)

$$\varepsilon = \left(\frac{Q_h - Q_c}{Q_c}\right) \times 100 \quad (1.3)$$

The deliberate heat loss from the test segment to the climate goes from 1.2% to 1.8%, which is fairly low. Condition (1.4) is utilized to process the typical heat transfer rate (Qavg) for both the hot and cold water sides to appraise the complete heat transfer coefficients:

$$Q_{avg} = \left(\frac{Q_c - Q_h}{Q_c}\right) \quad (1.4)$$

Using Equation (1.5), the surface area of the inner tube is determined.

$$A_i = \pi d_i L \quad (1.5)$$

The logarithmic mean temperature difference is calculated using the Equation (1.6)

$$\Delta T_{lm} = \frac{(T_{h1} - T_{c2}) - (T_{h2} - T_{c1})}{\mathrm{In}\left(\frac{T_{h1} - T_{c2}}{T_{h2} - T_{c1}}\right)} \quad (1.6)$$

The general heat transfer coefficient is determined utilizing the Condition (1.7).

$$U = \frac{Q_{avg}}{A_i \Delta T_{Im}} \quad (1.7)$$

The coefficient of annulus side heat transfer (ha) is calculated using the Dittus -Boelter (1930) Equation (1.8) correlation.

$$Nu_a = \frac{h_a - D_h}{k_c} = 0.023 Re_a^{0.8} Pr_c^{0.3} \quad (1.8)$$

5.1. Friction Factor

A pressure differential exists between the fluid and the tube wall (plain tape) when the fluid is moving through the tube at a specific velocity. Equation for a fully developed flow measures the frictional resistance, which is related to the pressure drop in the test section and is quantified by a quantity called the friction factor:

$$f = \frac{\Delta p}{\left(\frac{L}{d_i}\right)\left(\frac{pu^2}{2}\right)_h} \quad (1.9)$$

Using the U-tube manometer, the pressure drop (Δp) can be found and is estimated from the following Equation:

$$\Delta p = \left(p_{m-}p_{tf}\right) g\Delta h \quad (1.10)$$

6. CFD Modelling of Experimental Results

Computational fluid dynamics (CFD) uses mathematics to examine fluid movement, heat transport, and related processes. For the purpose of simulating and modelling mechanical, thermal, liquid, and gas flows, CFD solvers supply a complex collection of algorithms. Most technical advancements in the automotive, aeronautics, and space industries would be impossible to accomplish without CFD. Extensive study into the complete fluxes and heat exchange processes within the tube, as well as the development of technologies to increase heat transmission, was conducted using CFD modelling. Very little was written on doing simulations using a CFD for plain tape.

The current review utilized computational fluid dynamics (CFD) demonstrating with the ANSYSR15.0 code to gauge the heat transfer and rubbing factor for a plain tube and a tube fitted with Plain Tape, PT-SCA, PT-SCR, and PT-HW.

6.1. Computational Model

By treating the area around the heat exchanger's base as a fluid in ANSYS Fluent, we can study momentum and heat transfer. While solving for energy, the numerical solution models pressure decrease as a momentum sink and heat transfer as a heat source.

7. Performance Evaluation Analysis

An essential characteristic showing the possibility for practical uses of plain tape is the thermal enhancement factor, which is why it is analysed in this work. Each tape's thermal assessment is compared to the case without simple tape (plain tube) under continuous pumping power. The greater pressure drop that results from tube insertions is a trade-off for the improved heat transmission. Hence, to assess the net energy gain and find out if the shape of the plain tape used to boost heat transmission is beneficial from an energy perspective, a performance study

is crucial.

The proportion of the convective heat transfer coefficient of the plain tube to that of the tube with a tabulator is the meaning of the thermal upgrade factor (η) under consistent siphoning power. One way to put it is as:

$$\eta = \left|\frac{h_{tu}}{h_p}\right|_{pp} \qquad (1.11)$$

A thermal enhancement factor may be calculated in the following way using the Nusselt number correlation equation for a straight tube and its corresponding turbulator,

$$\eta = \left|\frac{h_{tu}}{h_p}\right|_{pp} = aRe^{-b} \qquad (1.12)$$

As the Reynolds number increases, the thermal enhancement factor falls, as seen in Equation (1.12). From an energy savings perspective, the thermal enhancement effect makes sense when its value is more than the sum of its components, indicating that the enhancing tool's influence on heat transfer is stronger than the growing friction factor's effect, and vice versa.

7.1. Plain Tape

The fluctuation of the thermal enhancement factor with respect to Reynolds number is demonstrated, and Equation (1.13) expresses it for plain tape, while Equations (1.2) and (1.3) represent it for laminar and turbulent flows, respectively.

$$\eta = 2.045878\ Re^{-0.05} \qquad (1.13)$$

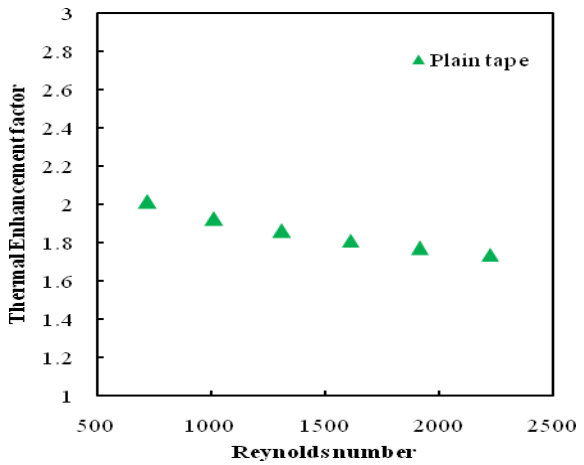

Figure 5: Thermal enhancement factors for Plain Tape in laminar flow versus Reynolds number

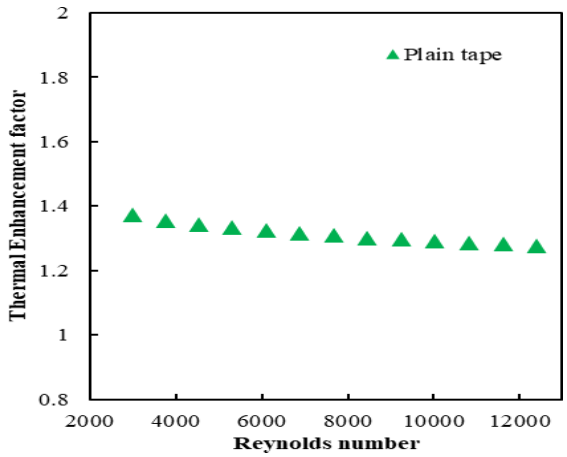

Figure 6: Thermal enhancement factors for Plain Tape under turbulent flow versus Reynolds number

It is observed that the thermal enhancement decreases with the increase in Reynolds number & it gives higher thermal enhancement than that of the plain tube.

7.2. Plain Tape Step Cut Arc (PT-SCA)

Thermal enhancement factors for the Plain tape with step cut arc (PT-SCA) inserted in plain tube are calculated and presented in provided Figures:

$$\eta = 2.02259 \ Re^{-0.03332} \qquad (1.14)$$

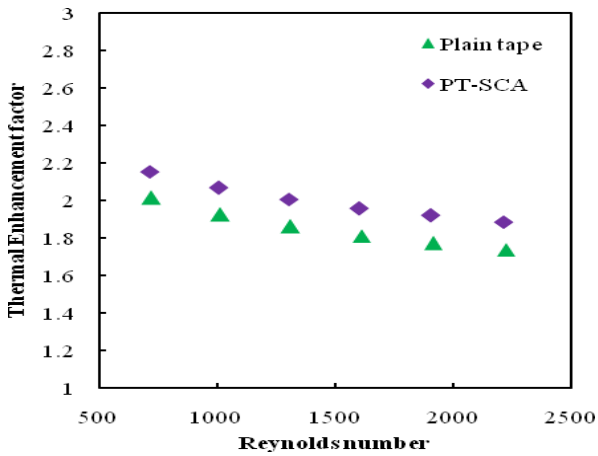

Figure 7: Thermal enhancement factors for PT-SCA and Plain Tape under laminar flow versus Reynolds number

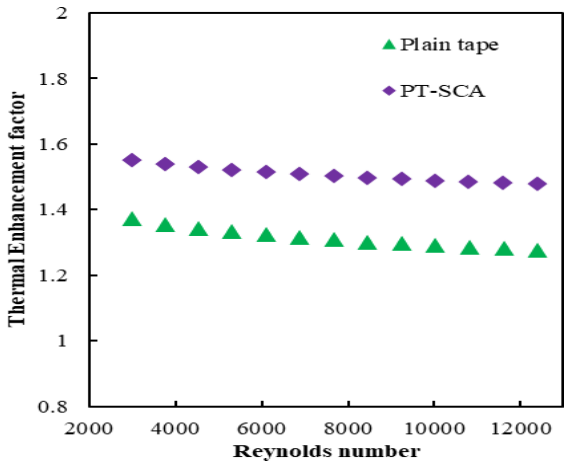

Figure 8: Thermal enhancement factors for PT-SCA and Plain Tape in turbulent flow versus Reynolds number

The data clearly show that as the Reynolds number increases, the thermal enhancement diminishes. At low Reynolds numbers, the thermal enhancement factor value is substantial across all examples in our investigation. Table 1 shows the comparison of the thermal enhancement factor of plain tape and plain tape with step cut arc (PT-SCA) inserts. Use of PT-SCA results in a stronger thermal enhancement effect than traditional plain tape.

Table 1: Factor of thermal enhancement for PT and PT-SCA

S. No	**Thermal enhancement factor (η)**			
	Laminar flow		**Turbulent flow**	
	PT	**PT-SCA**	**PT**	**PT-SCA**
1	1.739-2.015	1.886-2.155	1.276-1.370	1.477-1.549

7.3. Plain Tape Step Cut Rectangle (PT-SCR)

The equations for turbulent flows and laminar flows, respectively, provide the thermal enhancement factor for the plain tape step cut rectangle.

$$\eta = 2.001049\ Re^{-0.017781} \qquad (1.15)$$

The thermal enhancement for laminar flow and turbulent flow is compared in Figures 1 and 2, respectively, using Plain Tape and Plain Tape Step Cut Rectangle.

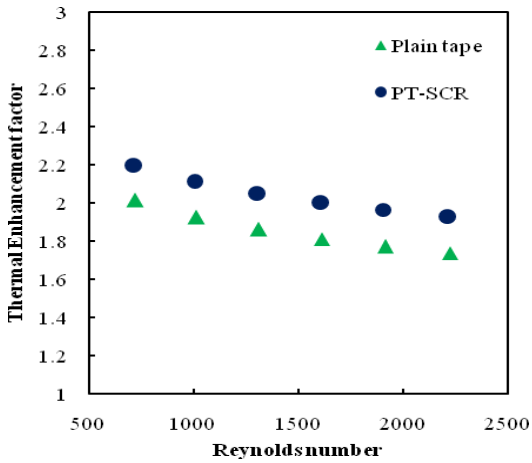

Figure 9: Thermal enhancement factors for PT-SCR and Plain Tape under laminar flow versus Reynolds number

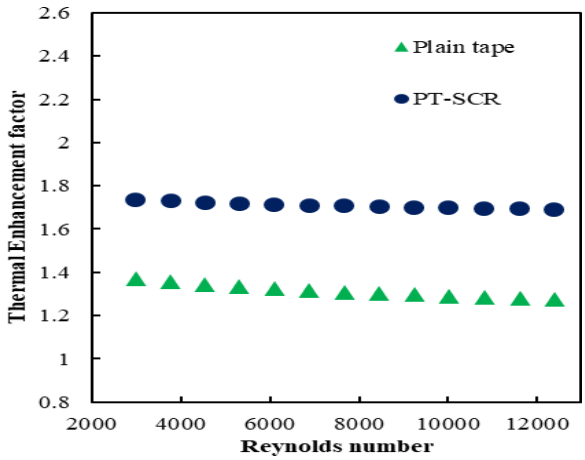

Figure 10: Thermal enhancement factors for PT-SCR and plain tape in turbulent flow versus Reynolds number

The thermal enhancement for Plain Tape & PT-SCR under laminar and turbulent flow are given in the Table 2.

Table 2 : Factor of thermal enhancement for PT-SCR and plain tape

S. No	**Thermal enhancement factor (η)**			
	Laminar flow		**Turbulent flow**	
	PT	**PT-SCR**	**PT**	**PT-SCR**
1	1.739-2.015	1.933-2.200	1.276-1.370	1.692-1.735

In the specified Reynolds number range, the experimental findings show that PT-SCR improves heat transmission even further than Plain Tape. Thermal enhancement also has a value greater than one in every instance. From an energy-savings perspective, it meant that the enhanced effect makes sense.

7.4. Plain Tape Horizontal Wing Cut (PT-HW)

What follows is the Given Equation that, in both turbulent and laminar flows, determines the thermal enhancement factors for PT-HW:

$$\eta = 1.987668\, Re^{-0.008} \qquad (1.16)$$

When it comes to laminar flow, the provided figures indicate how the Plain Tape performs, whereas the Plain Tape Step Cut Rectangle performs better in turbulent flow.

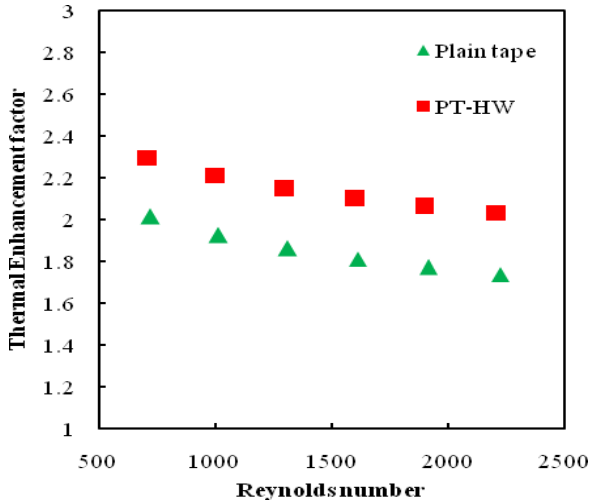

Figure 11: Thermal enhancement factors for PT-HW and Plain Tape under laminar flow versus Reynolds number

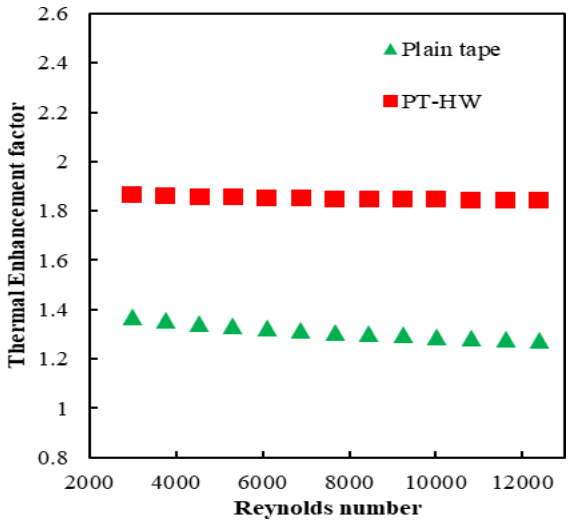

Figure 12: Thermal enhancement factors for PT-HW and Plain Tape in turbulent flow versus Reynolds number

Table 3: Factor of thermal enhancement for both PT and plain tape-HW

S. No	**Thermal enhancement factor (η)**			
	Laminar flow		**Turbulent flow**	
	PT	**PT-HW**	**PT**	**PT-HW**
1	1.739-2.015	2.035-2.296	1.276-1.370	1.842-1.864

The figures and tables provided earlier compare the thermal enhancement factors with PT-HW and Plain Tape. Thanks to its efficient turbulence mixing, PT-HW produced the best enhancement values compared to the other inserts. This was especially true when compared to Plain Tape in tube. At higher Reynolds numbers, the thermal enhancement factor is almost constant and tends to decrease with increasing Reynolds numbers.

8. Discussion

In this chapter, we examine the different plain tapes' thermal performance indicators, such as the Nusselt number and friction factor characteristics, by looking at their output data. As an alternative to comparing the cassettes individually, it would be more beneficial to compare the output with the thermal enhancement factor in the present study.

8.1. Laminar Flow

With respect to the Reynolds number, Figure 13 displays the relationship between different types of plain tapes utilized in the present laminar flow.

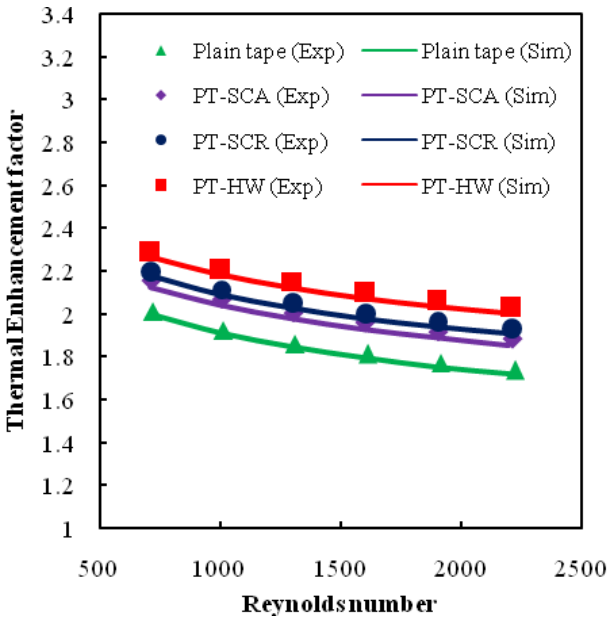

Figure 13: Reynolds number vs thermal enhancement factor in laminar flow103

8.2. Turbulent Flow

Figure 14 displays a comparison of the thermal enhancement factors of several flat tapes utilized in the present turbulent flow, organized by Reynolds number.

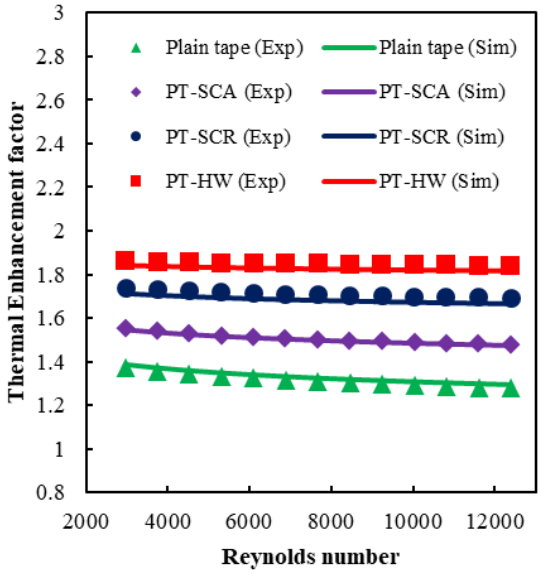

Figure 14: Under turbulent flow, thermal enhancement factor vs. Reynolds number

1. Plain tube

i. The experimental setup for laminar and turbulent flows was tested for efficiency using conventional correlations on the plain tube data of Nusselt number and friction factor. There was no statistically significant difference between the test and standard correlation values.

2. Plain Tape

i. For laminar flow, the plain tape thermal enhancement factor demonstrated a maximum divergence of 1.0090 times between analytical and experimental values, while for turbulent flow, it was 0.9866 times.

ii. The thermal boost provided by the plain tape was greater than that of the plain tube since the former generated more whirl flow than the latter did.

3. PT-SCA

i. Instead of employing simple tape or tube, inserts of different forms are utilised to get great performance. The amplification is caused by a minor incision on the tape's periphery, which disrupts the primary whirl flow even more, leading to the development of secondary flow.

ii. The plain tape with step cut arc outperformed the plain tube and plain tape in terms of thermal enhancement and overall performance in this study's comparisons.

iii. In laminar flow, the greatest deviation of the plain tape with step cut arc and plain tube on the thermal enhancement factor between the analytical and experimental data is 1.0147 times, and in turbulent flow, it is 1.0016 times.

4. PT-SCR

i. The Nusselt number and thermal enhancement factor of a plain tape with a step cut rectangle insert are much greater than those of plain tape, plain tube, and plain tape with a step cut arc. There is a greater disruption to the water flow at the plain tube due to the cutting region of this insert. The region around the insert has a cornering geometry, which increases the whirl flow.

ii. Better heat transmission is another benefit of narrowing the cut width and deepening it. Why? Because increasing the breadth of the cut while decreasing its depth produces less turbulence than promoting the vorticity behind the cut any more.

iii. In laminar flow, the greatest divergence between the analytical and experimental results for plain tape with step cut arc and plain tube on the thermal enhancement factor is 1.0105 times, while in turbulent flow, it is 1.0147 times.

5. PT-HW

i. The PT-HW outperforms alternative inserts for both laminar and turbulent flows in terms of thermal efficiency of the individual tubes because of the high degree of turbulences mixing near the trial tubing wall.

ii. Max deviations of turbulent and laminar streams entering the Plain Tube, along with experimental PT-HW data, are used to build this correlation between Nusselt's number and the

friction factor.

iii. In laminar flow, the greatest divergence between analytical and experimental findings for plain tape with step cut arc and plain tube on thermal enhancement factor is 1.0133 times, while in turbulent flow, it is 1.0130 times.

References

1. Wang, L., Xu, Y., Luo, W., & Li, W. (2020). Optimal design of double-layered microchannel heat sinks considering flow maldistribution and pressure drop using surrogate-based optimization. International Journal of Heat and Mass Transfer, 146, 119055. doi:10.1016/j
2. Wang, Q., Chen, R., Xu, Z., & Li, W. (2022). Design and optimization of microchannel heat exchangers for fuel cell systems using entropy generation minimization. International Journal of Heat and Mass Transfer, 177, 121609. doi: 10.1016/j.ijhmt.2021.121609
3. Wang, R., Zhang, F., Wang, F., & Zhao, X. (2021). Multi-objective optimization of shell-and-tube heat exchangers for cryogenic applications. Energy Conversion and Management, 240, 114305. doi: 10.1016/j.enconman.2021.114305
4. Xu, B., Yang, Y., Sun, Z., & Li, Z. (2023). Multi-objective optimization of shell-and-tube heat exchangers with helical baffles using an improved cuckoo search algorithm. International Journal of Refrigeration, 150, 152-168. doi: 10.1016/j.ijref.2023.05.005
5. Xu, Y., Zhou, Y., Liu, M., & Li, W. (2021). Performance analysis and multi-objective optimization of printed circuit heat exchangers for aerospace thermal management. Applied Thermal Engineering, 192, 116955. doi: 10.1016/j.applthermaleng.2021.116955
6. Zhang, F., Wang, H., & Zhao, X. (2020). Multi-objective optimization of spiral plate heat exchangers for cryogenic applications using NSGA-II. Applied Thermal Engineering, 174, 115139. doi: 10.1016/j.applthermaleng.2020.115139
7. Zhang, Y., Sun, Z., Li, W., & Li, Z. (2022). Design and optimization of microchannel heat exchangers for high-performance electronic cooling: A review. Renewable and Sustainable Energy Reviews, 159, 145-172. doi: 10.1016/j.rser.2022.02.022
8. Zhou, Y., Wu, Y., Xu, Z., & Li, W. (2020). Multi-objective optimization of plate-fin heat exchangers with wavy channels for low-temperature waste heat recovery. Applied Thermal Engineering, 178, 115865. doi: 10.1016/j.applthermaleng.2020.115865
9. Zhou, Y., Wu, Y., Xu, Z., & Li, W. (2021). Multi-objective optimization of finned tube heat exchangers with internal spiral ribs for thermal management of high-power LEDs. Applied Thermal Engineering, 198, 117296. doi: 10.1016/j.applthermaleng.2021.117296
10. Zhu, W., Zhang, S., & Li, W. (2020). Design and optimization of compact plate-fin heat exchangers for waste heat recovery in organic Rankine cycles. Applied Energy, 277, 115605. doi: 10.1016/j.apenergy.2020.115605
11. Chen, R., Wang, Q., Xu, Z., & Li, W. (2019). Optimization of plate-fin heat exchangers based on entropy generation minimization using a multi-objective genetic algorithm. International Journal of Heat and Mass Transfer, 130, 486-500. doi: 10.1016/j.ijhmt.2018.10.064
12. Cui, W., Li, S., & Ma, X. (2020). A review on numerical and experimental studies of shell-and-tube heat exchangers with helical baffles. Applied Thermal Engineering, 179, 115949. doi: 10.1016/j.applthermaleng.2020.115949
13. Li, J., Li, Z., Wu, Y., & Wang, L. (2018). Design and optimization of plate-fin heat exchangers for waste heat recovery in heavy-duty diesel engines. International Journal of Refrigeration, 95, 155-168. doi: 10.1016/j.ijref.2018.07.007
14. Li, L., Luo, W., & Yang, Y. (2019). Design and optimization of microchannel heat sinks for

high-heat-flux LED packaging using hybrid optimization algorithms. International Journal of Heat and Mass Transfer, 141, 118207. doi: 10.1016/j.ijhmt.2019.07.083

15. Tlili, F., Abidi, M. S., Ben Kirane, N., & Gabas, C. (2020). Multi-objective optimization of a plate and fin heat exchanger with hybrid nanofluids using response surface methodology. International Journal of Thermal Sciences, 155, 106570. doi: 10.1016/j.ijts.2020.05.025